

# Rapid passage signals from a vibrationally excited target molecule: a pump and probe experiment with continuous wave quantum cascade lasers

R. J. Walker,<sup>1</sup> J. H. van Helden,<sup>1</sup> J. Kirkbride,<sup>1</sup> E. A. McCormack,<sup>1</sup> M. T. Bell,<sup>1</sup>  
D. Weidmann,<sup>1,2</sup> and G. A. D. Ritchie<sup>1,\*</sup>

<sup>1</sup>Department of Chemistry, The Physical and Theoretical Chemistry Laboratory,  
The University of Oxford, South Parks Road, Oxford OX1 3QZ, UK

<sup>2</sup>Space Science & Technology Department, STFC Rutherford Appleton Laboratory,  
Harwell Science and Innovation Campus, Didcot, OX11 0QX UK

\*Corresponding author: grant.ritchie@chem.ox.ac.uk

Received July 19, 2011; accepted August 18, 2011;  
posted November 2, 2011 (Doc. ID 151331); published December 9, 2011

Two 5  $\mu\text{m}$  continuous wave quantum cascade lasers are used to perform a counterpropagating pump and probe experiment on a low pressure sample of nitric oxide. The strong pump field excites a fundamental rovibrational transition and the weaker probe field is tuned to the corresponding rotationally resolved hot band transition. When both light fields are in resonance, rapid passage is observed in the hot band absorption lineshape arising from a minimally damped and velocity-selected sample of molecules in the  $v = 1$  state. The measured rapid passage signals are well described by a two-level model based on the optical Bloch equations. © 2011 Optical Society of America  
OCIS codes: 300.6360, 300.6420, 300.1030, 020.3690.

The advent of single mode high power ( $>100$  mW) continuous wave (cw) quantum cascade lasers (QCLs) [1–3] opens up the possibility of using these sources for vibrational state preparation of molecules. In this Letter we present the first example, to our knowledge, of a pump and probe experiment in which a vibrationally excited molecule, nitric oxide ( $v = 1$ ), is prepared by an initial cw QCL, and then probed by a second cw QCL, which has been tuned to a rotationally resolved transition within the  $v = 2 \leftarrow 1$  hot band. The use of a cw QCL with a narrow linewidth allows sub-Doppler resolution and observation of a minimally damped rapid passage (RP) absorption lineshape associated with a velocity-selected rovibrational state.

The pump laser is a water-cooled external cavity QCL (Daylight Solutions) tunable over the range 1776–1958  $\text{cm}^{-1}$ , with a maximum output power of 140 mW and a beam waist of 2 mm. The linewidth of this laser is *c.a.* 2 MHz, determined from Lamb-dip spectroscopy [4,5]. The probe laser is a distributed feedback QCL (Alpes Lasers) covering the range 1818–1830  $\text{cm}^{-1}$  with maximum output power of 7 mW and a beam waist of 4 mm. This laser is mounted in a custom mechanical housing and driven using commercial current and temperature controllers (ILX Lightwave—models LDX-3232 and LDT-5545B). The linewidth of this probe laser cannot be determined directly as the power output is insufficient for Lamb-dip measurements. However, it is estimated to be *c.a.* 16 MHz on a millisecond timescale, which has been inferred from experiments measuring direct absorption spectra of NO with Doppler-limited lineshapes. The linewidth originates primarily from current ripple and noise introduced by the current source. The beams counterpropagate through a 70 cm long cell containing a low pressure of NO gas (10–200 mTorr). After passing through the cell, the pump and probe beams are focused using off-axis paraboloid mirrors onto thermoelectrically cooled mercury cadmium telluride detectors (VIGO PVI-2TE-6 and

PVMI-3TE-10.6, respectively), the outputs of which are then fed into an oscilloscope (LeCroy Wavesurfer 44MXsA), and stored for further processing.

The pump laser frequency is scanned across a range of *c.a.* 1 GHz at a rate selected in the range 10–100 Hz by modulating the PZT element on the laser's external cavity. The scan encompasses both  $\Lambda$ -doublet components of the  $R(6.5)_{1/2}$  rotational transition in the  $v = 1 \leftarrow 0$  band, as depicted in Fig. 1(a). In contrast, the probe laser is scanned at much higher rates, in the range 1 kHz–200 kHz, so that the effect of collisional population transfer from the initially prepared rovibrational state is minimized. The probe is tuned over *c.a.* 6.5 GHz which allows both  $\Lambda$ -doublet components of the  $P(7.5)_{1/2}$  transition of the  $v = 2 \leftarrow 1$  band to be observed. The polarizations of the pump and probe lasers were initially crossed, with a horizontally polarized pump and a vertically polarized probe laser. Changing the pump polarization with a  $\lambda/2$  waveplate increased the magnitude of the transient signal by a factor of 1.5, while a  $\lambda/4$  waveplate had no apparent effect. Changing polarizations did not affect the form of the signal apart from its magnitude, and as such the additional optics were removed to reduce etalons.

Figure 1(a) shows a time record of the transmission signals observed from an experiment using 30 mTorr of NO when the pump laser is scanned over the fundamental transitions and the probe is much more rapidly scanned (chirp rate of 0.13  $\text{MHz ns}^{-1}$ ). Figure 1(b) and 1(c) show sections of the probe beam signals for two different pump laser frequencies, respectively on and off resonance with the rotational transition. Figure 1(b) exhibits no specific features within the probe signal whereas Fig. 1(c) shows a single spectral signature across the probe scan range. This spectral signature could be seen to change position within the probe laser scan over the course of the pump laser scan. This behavior is expected as the velocity subset of the

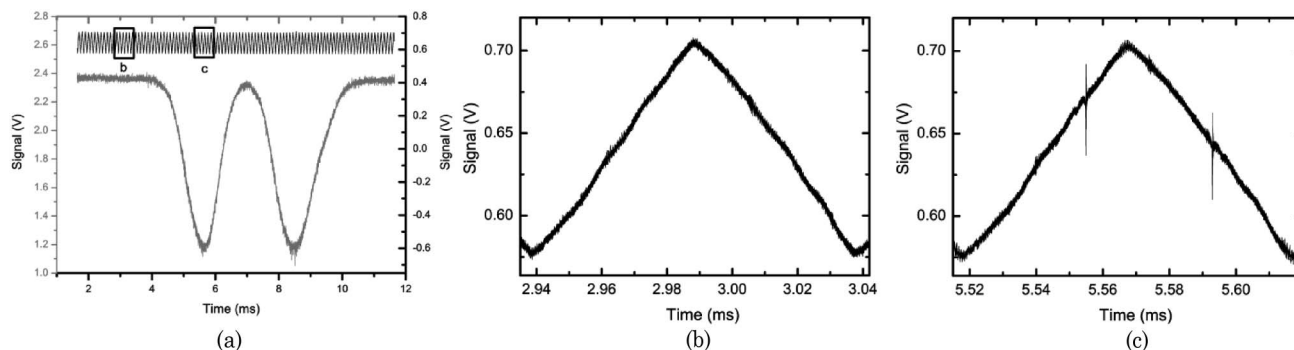


Fig. 1. Experimental transmission spectra showing (a) light detected from pump (gray) and probe (black) lasers on the same timescale, note cutaways b and c showing, (b) probe laser scan when the pump laser is off resonance with the  $R(6.5)_{1/2}$  transition of the  $v = 1 \leftarrow 0$  band, (c) probe laser scan when pump laser is on resonance with the  $R(6.5)_{1/2}$  transition of the  $v = 1 \leftarrow 0$  band.

Maxwell-Boltzmann distribution that is pumped varies and, more obviously, as each of the  $\Lambda$ -doublet resolved transitions is pumped in turn.

Figure 2 shows in detail the probe signal observed when the pump laser is on resonance. In order to improve the signal to noise of the data, particularly at the tail of the transient, 80 signal traces at pump resonance were averaged. Before averaging, the spectra were realigned onto the most intense peak in order to compensate for small probe laser frequency drifts induced by the current controller. The observed signal spans  $\sim 200$  ns, equivalent to a  $\sim 26$  MHz range at this chirp rate, which is smaller than the room temperature Doppler FWHM of 124 MHz, indicating that velocity-selected pumping has been achieved. The signal exhibits marked oscillatory structure, which always occurs postresonance, later in time during the scan, and is unaffected by the chirp direction of the probe laser. It can be seen that as the probe laser is swept through the resonance the relative frequency of the oscillations increases with time. Changing the laser intensity of the pump or probe laser beams only affects the absolute magnitude of the signal, proving that the oscillatory structure is not caused by Rabi oscillations. It is therefore attributable to RP in which the polarized vibrationally excited sample interferes with the

chirped probe laser on a timescale that is shorter than typical relaxation processes for the system.

In order to model the RP signals, the Maxwell-Bloch equations were used to calculate the expected transmission of the probe beam through the gas sample. The spatial dependence of the electric field and its phase along the 70 cm path length is calculated using a spectral method based on Chebyshev grid points [6], with the response of the gas medium at each of the grid points determined by solving the optical Bloch equations. The Bloch vectors are propagated in a retarded time reference frame using the analytical expressions for a driven two-level system with relaxation, given by Torrey [7]. A Gauss-Hermite quadrature is used to integrate the Bloch vectors for different molecular velocities, where, in order to take into account the velocity selection occurring, the Doppler width of the transition was modified to reflect the 2 MHz linewidth of the pump beam. Further averaging is performed to account for the magnetic quantum number dependence of the transition dipole moment with respect to the laser polarization. By assuming the population transfer from  $v = 1 \leftarrow 0$  is 16%, which is consistent with a saturation parameter of 0.5, previously determined for these experimental conditions [4], the response of 30 mTorr of NO for a probe chirp rate of  $0.13 \text{ MHz ns}^{-1}$  is simulated. The resulting signal is convoluted with a Gaussian function with a FWHM corresponding to the detector time response (10 ns). Clearly, the experimental signal is well-reproduced by the simulation in Fig. 2, confirming the occurrence of RP in this system.

The decaying oscillations of the RP signals are well fit by the following functional form

$$A(t) = A_0 e^{-t/\tau} \sin(\mu t^2), \quad (1)$$

in which  $A_0$  is the magnitude of the signal,  $\tau$  is the decay time, and  $\mu$  is half of the angular frequency chirp rate [8]. Experimental signals are fit by Eq. (1) in order to extract the decay time,  $\tau$ . A Nelder-Mead simplex algorithm was utilized and the errors in the fitting parameters calculated from the square roots of the diagonals of the covariance matrix. Figure 3 shows the measured variation of  $\tau$  with pressure of NO. As expected,  $\tau$  reduces with increasing pressure of the chromophore as the increased collision frequency leads to more rapid dephasing and relaxation of the induced polarization. Interestingly,  $\tau$  reaches a

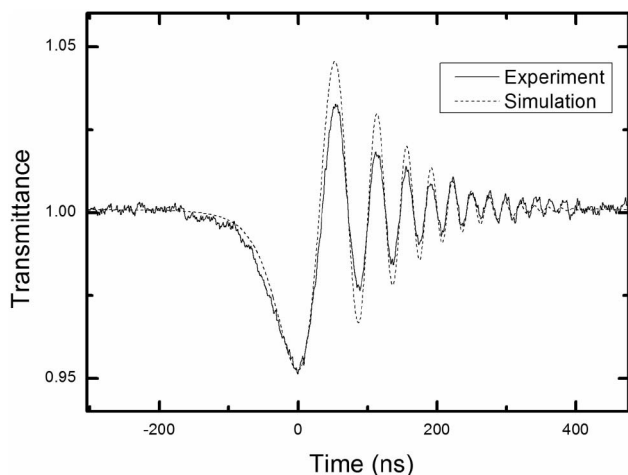


Fig. 2. Comparison of experimental and simulated velocity-selected RP signals for 30 mTorr of NO and a chirp rate of  $0.13 \text{ MHz ns}^{-1}$ .

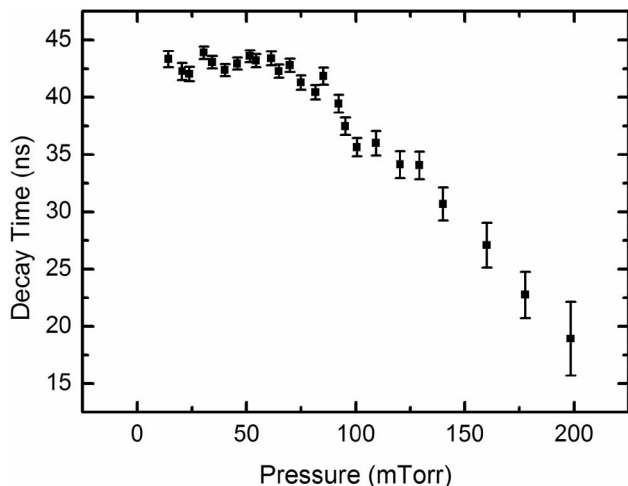


Fig. 3. Decay times retrieved from the fitting of experimental RP signals with Eq. (1) as a function of the pressure of NO. The data are averaged over both  $\Lambda$ -doublet components of the  $P(7.5)_{1/2}$  transition of the  $v = 2 \leftarrow 1$  band and over both up and down frequency scans.

plateau indicating that the dephasing of the induced polarization at low pressures is not limited by collisional effects, but most likely by the spread in molecular velocity components being sampled, and the probe laser linewidth. We emphasize, however, that the measured limiting value for  $\tau$  is both chirp rate and detector-response dependent.

We note that our measurements use a relatively slowly scanned probe laser (*c.a.*  $0.1\text{--}0.8\text{ MHz ns}^{-1}$ ), at least 2 orders of magnitude less than those achieved with typical pulsed QCL systems [9]. Such slow chirp rates would not normally allow RP signals to be observed. Indeed, in an experiment without the pump laser in which the probe laser is tuned to the nearby  $P(14.5)_{3/2}$  transition in the  $v = 1 \leftarrow 0$  band, no RP is perceptible and a Doppler-limited lineshape convoluted with the 16 MHz linewidth of the probe laser is observed. As such, it is the use of two sub-Doppler laser bandwidths that enables resolution of the RP signals; the measurements are made on a sub- $\mu\text{s}$  timescale and so collisions do not induce fast dephasing and relaxation in the system, such that the RP signal persists. If the gas pressure is increased to 100 mTorr, the probe signals change as shown in Fig. 4. Here collisional transfer of population from the initially prepared state into the nearly degenerate  $\Lambda$ -doublet state of opposite parity is readily observed, as has been reported in the literature for  $v = 2$  [10].

The replacement of the low power probe with a higher power system (*c.a.* 100 mW) offers the enticing prospect of using a stimulated Raman adiabatic passage

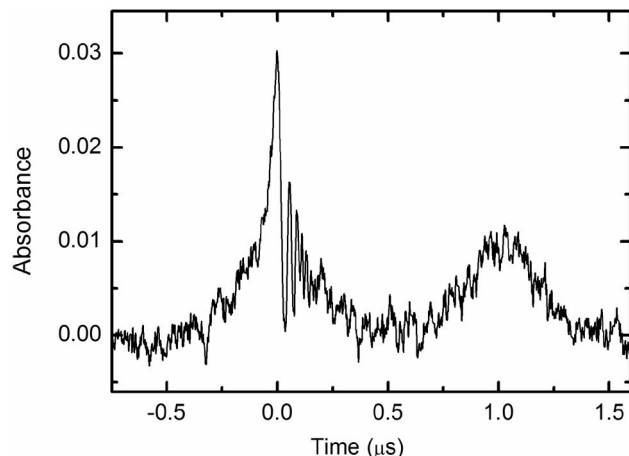


Fig. 4. Hot band spectra taken at 100 mTorr of NO. At these higher pressures population can be seen to scatter into a range of velocity states as well as the neighboring near-degenerate  $\Lambda$ -doublet component.

methodology to prepare significant population in the  $v = 2$  level [11,12].

This work is conducted under the Engineering and Physical Sciences Research Council programme grant EP/G00224X/1: New Horizons in Chemical and Photochemical Dynamics. R. J. Walker and J. Kirkbride would like to thank the EPSRC for the award of postgraduate studentships.

## References

1. R. F. Curl, F. Capasso, C. Gmachl, A. A. Kosterev, B. McManus, R. Lewicki, M. Pusharsky, G. Wysocki, and F. K. Tittel, *Chem. Phys. Lett.* **487**, 1 (2010).
2. J. Faist, F. Capasso, D. L. Sivco, C. Sirtori, A. L. Hutchinson, and A. Y. Cho, *Science* **264**, 553 (1994).
3. F. Capasso, *Opt. Eng.* **49**, 111102 (2010).
4. G. Hancock, G. Ritchie, J.-P. van Helden, R. Walker, and D. Weidmann, *Opt. Eng.* **49**, 111121 (2010).
5. R. J. Walker, J. H. van Helden, and G. A. D. Ritchie, *Chem. Phys. Lett.* **501**, 20 (2010).
6. L. N. Trefethen, *Spectral Methods in MATLAB* (SIAM, 2000).
7. H. Torrey, *Phys. Rev.* **76**, 1059 (1949).
8. V. V. Khodos, D. A. Ryndyk, and V. L. Vaks, *Eur. Phys. J. Appl. Phys.* **25**, 203 (2004).
9. M. T. McCulloch, G. Duxbury, and N. Langford, *Mol. Phys.* **104**, 2767 (2006).
10. M. Islam, I. W. M. Smith, and M. H. Alexander, *Phys. Chem. Chem. Phys.* **2**, 473 (2000).
11. S. M. Hamadani, A. T. Mattick, N. A. Kurnit, and A. Javan, *Appl. Phys. Lett.* **27**, 21 (1975).
12. N. Mukherjee and R. N. Zare, *Chem. Phys. Chem.* **132**, 154302 (2010).